



# Highly dispersed carbon nanotube reinforced cement based materials

Maria S. Konsta-Gdoutos<sup>a,\*</sup>, Zoi S. Metaxa<sup>a,b</sup>, Surendra P. Shah<sup>b</sup>

<sup>a</sup> Department of Civil Engineering, Democritus University of Thrace, Xanthi, Greece

<sup>b</sup> Center for Advanced Cement-Based Materials, Northwestern University, Evanston, Illinois, USA

## ARTICLE INFO

### Article history:

Received 10 December 2008

Accepted 28 February 2010

### Keywords:

Carbon nanotubes

Dispersion<sup>A</sup>

Mechanical properties<sup>C</sup>

Scanning electron microscopy (SEM)<sup>B</sup>

Fiber reinforcement<sup>E</sup>

## ABSTRACT

The remarkable mechanical properties of carbon nanotubes (CNT) suggest that they are ideal candidates for high performance cementitious composites. The major challenge however, associated with the incorporation of CNTs in cement based materials is poor dispersion. In this study, effective dispersion of different length multiwall carbon nanotubes (MWCNTs) in water was achieved by applying ultrasonic energy and in combination with the use of a surfactant. The effects of ultrasonic energy and surfactant concentration on the dispersion of MWCNTs at an amount of 0.08 wt.% of cement were investigated. It is shown that for proper dispersion the application of ultrasonic energy is absolutely required and for complete dispersion there exists an optimum weight ratio of surfactant to CNTs. For a constant ratio of surfactant to MWCNTs, the effects of MWCNT type (short and long) and concentration on the fracture properties, nanoscale properties and microstructure of nanocomposite materials were also studied. Results suggest that MWCNTs improve the nano- and macromechanical properties of cement paste.

© 2010 Elsevier Ltd. All rights reserved.

## 1. Introduction

A significant portion of the current civil infrastructure is partially or completely constructed out of cementitious materials such as concrete. Cementitious materials are typically characterized quasi-brittle materials with low tensile strength and low strain capacity. Fibers can be incorporated into cementitious matrices to overcome these weaknesses. Typical reinforcement of concrete is provided using reinforcing bars and macrofibers, both of which reinforce concrete on the millimeter scale. Recently, the use of microfiber reinforcement has led to significant improvement of the mechanical properties of cement based materials [1]. However, while microfibers delay the development of formed microcracks they do not stop their initiation. The development of new nanosized fibers has opened a new field for nanosized reinforcement within concrete [2]. The incorporation of fibers at the nanoscale will allow the control of the matrix cracks at the nanoscale level and essentially create a new generation of a “crack free material” [3,4].

Carbon nanotubes (CNTs) are considered one of the most beneficial nanomaterials for nano-reinforcement. The unique mechanical, electrical and chemical properties of CNTs make them an attractive candidate for reinforcement of composite materials. The Young's modulus of an individual nanotube should be around 1 TPa and its density is about 1.33 g/cm<sup>3</sup> [5]. Molecular mechanic simulations suggested that CNTs' fracture strains were between 10% and 15%,

with corresponding tensile stresses on the order of 65 to 93 GPa [6]. Their aspect ratios are generally beyond 1000.

Earlier attempts have been made to add CNTs in cementitious matrices at an amount ranging from 0.5 to 2.0 wt.% (by weight of cement) [7–12]. However, CNTs form agglomerates or bundles that are tightly bound because of the way they are produced. The major challenge associated with the incorporation of CNTs in cement based materials is poor dispersion [13]. Poor dispersion of CNTs leads to the formation of many defect sites in the nanocomposite and limits the efficiency of the CNTs in the matrix [14]. Scanning Electron Microscopy (SEM) images of poorly dispersed multiwall carbon nanotubes (MWCNTs) forming bundles in 18 h cement paste are shown in Fig. 1.

Prior work on CNTs in liquid dispersions has focused on pre-treatment of the nanotube's surface via chemical modification. Makar et al. [7] reported an ethanol/sonication technique for dispersing CNTs in cement. The results obtained from SEM and Vickers hardness measurements indicate that CNTs affect the early hydration progress, producing higher hydration rates. Li et al. [8,9] employed a carboxylation procedure to improve the bonding between MWCNTs and cement matrix and obtained modest improvements in compressive and flexural strength. Saez de Ibarra et al. [10] used gum Arabic as a dispersing agent and reported modest gains in compressive strength and Young's modulus. Wansom et al. [11] investigated the electrical properties of CNT-cement nanocomposites using a polycarboxylate based superplasticizer and methylcellulose. More recently, in order to obtain homogenous dispersions of MWCNTs in water, Cwirzen et al. [12] used polyacrylic acid polymers and sonication. The results showed a slight increase in compressive strength.

\* Corresponding author. Tel.: +30 25410 79658; fax: +30 25410 79652.

E-mail address: [mkonsta@civil.duth.gr](mailto:mkonsta@civil.duth.gr) (M.S. Konsta-Gdoutos).

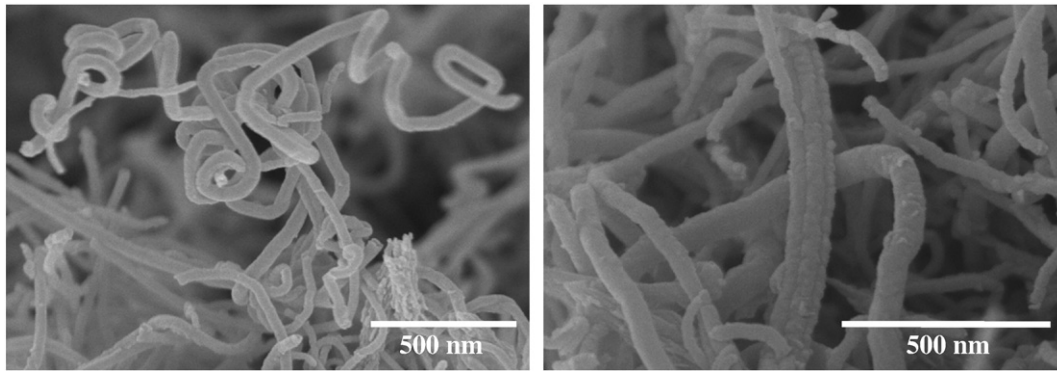


Fig. 1. SEM images of poorly dispersed MWCNTs forming bundles in 18 h cement paste.

In this study, the characteristics of cement paste reinforced with multiwall carbon nanotubes (MWCNTs) were investigated. Effective dispersion of MWCNTs in water was achieved by applying ultrasonic energy and in combination with the use of a surfactant. Two different types of MWCNTs having the same production method, the same diameter, but different lengths (designated as short and long), were used (Table 1). As length plays a key role on the dispersion of CNTs, the effect of ultrasonic energy on the dispersion of MWCNTs was investigated at first, measuring the rheological properties (viscosity) of cement paste reinforced with the long MWCNTs. The effect of the surfactant concentration on the fracture properties and the microstructure of nanocomposites reinforced with 0.08 wt.% of cement long MWCNTs was also studied. Moreover, the influence of MWCNT type (short versus long) and the effect of the concentration of MWCNTs on the fracture properties of the nanocomposites were studied for a constant weight ratio of surfactant to MWCNTs. SEM was employed to study the morphology and the microstructure of the cementitious nanocomposites. Finally, nanoindentation tests were conducted in order to examine the nanomechanical properties of the MWCNTs cementitious nanocomposites and to further investigate the large increase of the Young's modulus.

## 2. Experimental study

### 2.1. MWCNT suspension preparation

The cementitious material used in this study was ordinary Portland cement. Purified multiwall carbon nanotubes (MWCNTs) were used as received. Experiments were conducted with two different types of MWCNTs having the same production method, the same diameter, but different lengths, designated as short and long. The length of the short MWCNT was in the range of 10–30  $\mu\text{m}$  while the length of the long MWCNT was in the range of 10–100  $\mu\text{m}$  (Table 1). For the preparation of MWCNT dispersions, a surfactant (SFC) was used. In a typical procedure, suspensions were prepared by mixing the MWCNTs in an aqueous solution containing different amounts of surfactant and the resulting dispersions were sonicated at room temperature. Constant energy was applied to the samples using a 500 W cup-horn high intensity ultrasonic processor with a cylindrical tip and temperature controller. The sonicator was operated

at an amplitude of 50% so as to deliver an energy of 1900–2100 J/min at cycles of 20 s in order to prevent overheating of the suspensions.

### 2.2. Testing procedures

The influence of MWCNT dispersion on the rheological properties of cement paste samples was investigated. The rheological characteristics of the samples with the sonicated dispersions were measured using a Haake Rheostress 150 rheometer with a 20 mm concentric cylinder measurement system. A steady stress protocol similar to the one proposed by Yang et al. [15] was applied to determine the viscosity dependence on stress. Cement paste was placed in the rheometer immediately after mixing. Each sample was presheared at  $100 \text{ s}^{-1}$  for 200 s, and then allowed to rest for 200 s. A low stress of 4.5 Pa was applied to the sample, and the stress was increased stepwise using the protocol shown in Fig. 2. Initial stresses were chosen to be higher than the yield stress of the material. The samples were held at each stress condition for 40 s. The holding time was necessary to ensure that an equilibrium flow had been reached. Apparent viscosity ( $\eta$ ) as well as shear rate ( $\dot{\gamma}$ ) as a function of time was monitored and recorded during the test. The viscosity at each shear stress was obtained by averaging the values in the last 10 s that corresponded to the equilibrium region.

The morphology and the microstructure of the fracture surface of MWCNT reinforced nanocomposites were examined using two different types of ultra-high resolution field emission scanning electron microscopes (Hitachi S5500 and LEO Gemini 1525) operated at 3 to 5 kV. Secondary electron (SE) imaging was employed to obtain clear images at medium to high magnifications (10,000 $\times$  to 150,000 $\times$ ). Specimens of 25.4 $\times$ 6.35 $\times$ 6.35 mm were prepared for each mix. After the sonication, cement was added into the MWCNT suspensions at a water to cement ratio w/c = 0.5 by weight. The materials were mixed according to ASTM 305 using a standard Hobart mixer. After 18 h of curing, specimens were demolded and kept in

Table 1  
Properties of multiwall carbon nanotubes (MWCNTs).

	Aspect ratio	Diameter (nm)	Length ( $\mu\text{m}$ )	Purity (%)	Surface area ( $\text{m}^2/\text{g}$ )
Short	700	20–40	10–30	>95	110
Long	1600	20–40	10–100	>97	250–300

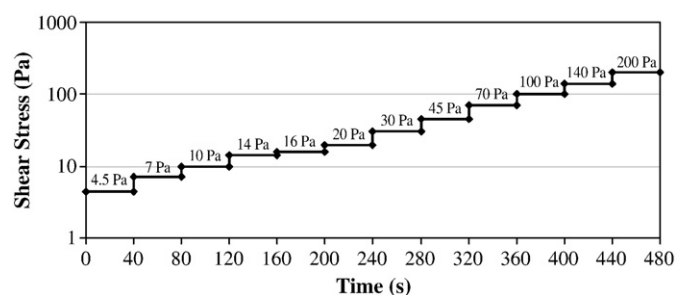


Fig. 2. Rheology measuring protocol.

acetone to stop the hydration. Prior to their observation, the fracture surface of the specimens was sputter-coated using the Denton Desk III system. Due to the roughness of the surface, a 20 nm thick layer of gold–palladium (Au/Pd) was used to eliminate charging effects caused by insufficient coating.

The mechanical performance of the MWCNT cementitious nanocomposites was evaluated by fracture mechanics tests. Beam specimens of  $20 \times 20 \times 80$  mm, prepared using the mixing protocol described previously, were tested by three-point bending at the age of 3, 7 and 28 days, as illustrated in Fig. 3. Three replications were made for each nanocomposite tested. Before testing a 6 mm notch was introduced to the specimens using a water-cooled diamond saw. The test was performed using an 89 kN, MTS servo-hydraulic, closed-loop testing machine. A clip gauge was used to measure the crack mouth opening displacement (CMOD). The CMOD was used as a feedback to produce a stable fracture at a rate of 0.012 mm/min. The load and the CMOD were recorded during the test. The ASTM C348 was followed to determine the average values of the flexural strength and Young's modulus. The specimens that result in strengths differing by more than 10% from the average value of all test specimens made from the same sample and tested at the same period were not considered in determining the flexural strength. After discarding the strength values, if less than two strength values were left for determining the flexural strength at any given period a retest was made. Following the above mentioned procedure assures that the variations of the test results are not significant and do not affect the conclusions. The Young's modulus was calculated from the load versus CMOD results using the two-parameter fracture model by Jenq and Shah [16].

The nanomechanical properties of the MWCNT composites were investigated using a triboindenter. The triboindenter is a special type of nanoindenter that combines nanoindentation to determine the local properties of the material at the nanoscale, with high resolution in-situ scanning probe microscopy (SPM) imaging that allows pre- and post-test observation of the sample. A Berkovich tip with a total included angle of  $142.3^\circ$  was used for indentation and SPM imaging. Multiple cycles of partial loading and unloading were used to make each indentation, eliminating creep and size effects [17]. The Oliver and Pharr method was used to determine the mechanical properties, where the indentation modulus is calculated from the final unloading curve [18]. Prismatic specimens of  $25.4 \times 6.35 \times 6.35$  mm were prepared and cured in water saturated with lime for 28 days. After curing, specimens were kept in acetone. Before testing, thin sections of approximately 5 mm were cut out of the specimens and mounted using an adhesive (softening temperature  $71^\circ\text{C}$ ) on a metal sample holder for polishing. Polishing is very important for nanoindentation. Eliminating the

sample roughness without any damage is necessary for the determination of reliable local mechanical properties [19]. Samples were polished using silicon carbide paper discs of gradation  $22\ \mu\text{m}$ ,  $14\ \mu\text{m}$ ,  $8\ \mu\text{m}$  and  $5\ \mu\text{m}$  and diamond lapping films of gradation  $6\ \mu\text{m}$  and  $3\ \mu\text{m}$ . Water was used in the first two and last two gradations. At every step an optical microscope was used to check the effectiveness of the polishing. As a final step the polished samples were ultrasonically cleaned in water for 1 min using a bath sonicator to remove polishing debris. An environmental scanning electron microscope (ESEM) at low vacuum mode was used to further investigate the effectiveness of the polishing procedure and find representative areas of the samples. Before nanoindentation, representative areas of the nanocomposites were also imaged using the Berkovich tip of the triboindenter to provide surface information at millimeter to nanometer scale. Nanoindentation was performed in a  $12 \times 12$  grid ( $10\ \mu\text{m}$  between adjacent grid points). This procedure was repeated in at least two different areas on each sample. Some of the nanoindentation data were discarded due to the irregular nature of the load-displacement plot, which could be due to the presence of large voids or cracking in the material [19].

### 2.3. Safety precautions handling CNTs

Since lately there is considerable concern about the impact of nanoparticles, including CNTs, on human health and the environment, it is only mandatory to address the safety precautions taken using CNTs. Although, based on the manufacturer's material data sheet, MWCNTs as received are considered as non-hazardous, the preparation and testing of both MWCNTs suspensions and cementitious samples were conducted in fume hoods using appropriate safety precautions, such as government approved respirators, compatible chemical-resistant gloves, safety goggles and protective work clothing. Additionally, all test equipments and machinery were cleaned thoroughly, and disposal of the samples took place following the university policy for handling hazardous materials.

## 3. Results and discussion

### 3.1. Effect of ultrasonic energy

Ultrasonication is a common physical technique used to disperse CNTs into base fluids [20,21]. Ultrasonic processors convert line voltage to mechanical vibrations. These mechanical vibrations are transferred into the liquid by the probe creating pressure waves. This action causes the formation and violent collapse of microscopic bubbles. This phenomenon, referred to as cavitation, creates millions

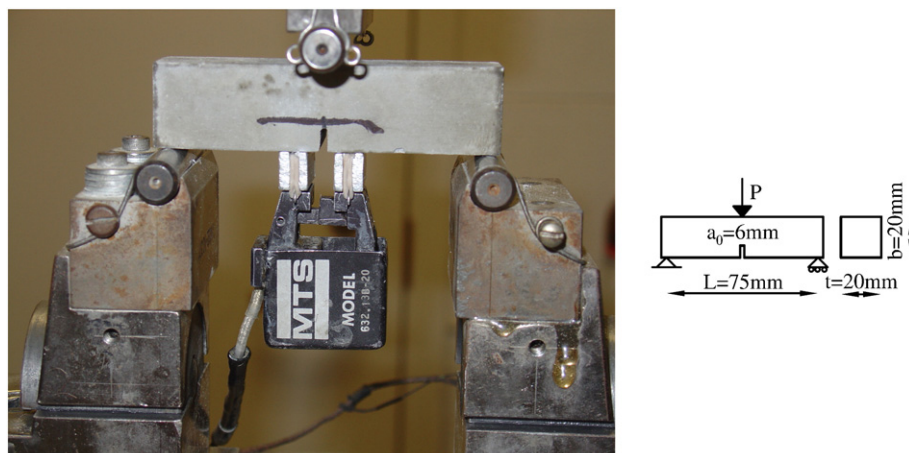


Fig. 3. Three-point bending test set up and configuration.



of shock waves, increasing the temperature in the liquid [21]. The cavitation collapse lasts only a few microseconds. Although the amount of energy released by each individual bubble is small, the cumulative effect causes extremely high levels of energy to be released, resulting in dispersion of objects and surfaces within the cavitation field.

The effect of ultrasonic energy on the dispersion of the CNTs was investigated measuring the rheological properties of cement paste samples reinforced with MWCNTs under steady shear stress. Rheology is a method commonly used to study the dispersion of CNTs suspensions. Under low shear stress, CNT agglomerates control the viscosity of the suspensions. Therefore, suspensions with larger scale agglomerates exhibit higher viscosity [15].

Results of preliminary rheological experiments have indicated that MWCNTs with greater length are more difficult to disperse. In this work, four different long MWCNTs (diameter 20–40 nm, length 10–100  $\mu\text{m}$ ) aqueous-surfactant suspensions were studied with surfactant to MWCNT weight ratios of 1.5, 4.0, 5.0 and 6.25. The MWCNTs' content was kept constant in the solution at an amount of 0.16 wt.% of water. Two mixes were prepared for each surfactant to MWCNT ratio, one with the use of ultrasonic energy and one without. Then the suspensions were mixed with cement and the rheological properties of the cementitious composite samples were investigated using the mixing and measuring protocol described previously.

Fig. 4 shows the behavior of cementitious nanocomposites ( $w/c = 0.5$ ) reinforced with long MWCNTs using a surfactant to CNTs ratio of 6.25. Two different suspensions are presented: those of MWCNTs treated with sonication energy, (CP + SFC + MWCNTs sonicated), and those without, (CP + SFC + MWCNTs). The results are compared to the plain cement paste containing the same amount of surfactant (CP + SFC). All samples exhibit the typical shear thinning response of cement paste. At low shear stress the viscosity is high while at high shear stress ( $>70$  Pa) the viscosity is decreasing and reaches a “plateau” region in which the fluid seems to have a constant viscosity. It is observed that the dispersions without sonication exhibit viscosity at low stress (14 Pa) of up to 0.13 Pa s while the sonicated dispersions exhibit viscosity of 0.09 Pa s which is very close to the viscosity of plain cement paste (0.07 Pa s). As expected, at low stress conditions the application of ultrasonic energy controls the dispersion of the MWCNTs. Under high shear stress ( $>70$  Pa) the agglomerates can be broken down by the fluid motions so the viscosities of the suspensions with and without sonication are similar. Analogous results (shown in Table 2) were obtained with a surfactant to MWCNT ratio of 1.5, 4.0 and 5.0. Based on those results it can be concluded that for proper dispersion the application of ultrasonic energy is required.

### 3.2. Surfactant concentration effect

In order to investigate the surfactant concentration effect on the dispersion of the MWCNTs, nanoimaging of the fracture surfaces and fracture mechanics tests of samples with surfactant to long MWCNTs (diameter 20–40 nm, length 10–100  $\mu\text{m}$ ) at weight ratios of 0, 1.5, 4.0,

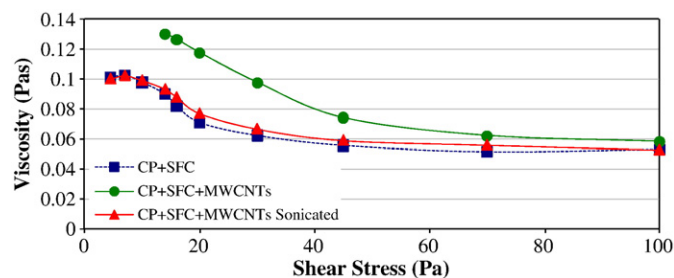


Fig. 4. Steady shear viscosity of cement paste ( $w/c = 0.5$ ) reinforced with long MWCNTs.

Table 2

Viscosities (Pa s) at low shear stress condition of cement paste ( $w/c = 0.5$ ) reinforced with MWCNTs.

Surfactant/CNT weight ratio	1.5	4.0	5.0
CP + SFC	0.86	0.27	0.20
CP + SFC + MWCNTs	0.94	0.39	0.26
CP + SFC + MWCNTs sonicated	0.89	0.29	0.20

5.0, 6.25 and 8.0 were performed. Cement paste samples ( $w/c = 0.5$ ) reinforced with 0.08 wt.% MWCNTs treated with different amounts of surfactant were prepared following the mixing protocol described previously.

Results from SEM images at a 1  $\mu\text{m}$  scale are presented in Fig. 5. As expected, in the samples where dispersion was achieved without the use of surfactant [Fig. 5(a)], MWCNTs appear poorly dispersed in cement paste, forming large agglomerates and bundles. In the case where dispersion was achieved with a surfactant to MWCNT ratio of 1.5 [Fig. 5(b)], it is observed that MWCNTs mainly remain as large agglomerates entangled in the cement paste hydration products. In that case, only a small amount of MWCNTs was dispersed. In samples where the surfactant to MWCNT ratio lies within the range from 4.0 to 6.25 [Fig. 5(c–d)], only individual MWCNTs were identified on the fracture surface.

The average values of maximum fracture load for cement paste samples containing long MWCNTs with different surfactant to MWCNT ratios for 28 days are plotted in Fig. 6. It is observed that samples treated with different amounts of surfactant exhibit higher fracture load than the sample with no surfactant. The samples with surfactant to MWCNT ratio of 4.0 give a higher average load increase at all ages. Surfactant to MWCNT ratios either lower or higher than 4.0 produce specimens with less load increase. A possible explanation could be that at lower surfactant to MWCNT ratios, less surfactant molecules are absorbed to the carbon surface and the protection from agglomeration is reduced. At higher surfactant to MWCNT ratios, bridging flocculation can occur between the surfactant molecules. Too large amount of surfactant in the aqueous solution is causing the reduction of the electrostatic repulsion forces between the MWCNTs [20]. The results indicate that for effective dispersion, there exists an optimum weight ratio of surfactant to MWCNTs close to 4.0.

### 3.3. Effect of different types of MWCNTs and concentration

To evaluate the performance of different types (short and long) of MWCNTs, nanoimaging of the fracture surfaces of the cementitious nanocomposites and fracture mechanics tests were performed. Cement paste samples reinforced with lower and higher concentrations of MWCNTs (0.048 wt.% and 0.08 wt.%, respectively), treated at a constant surfactant to MWCNT weight ratio of 4 were prepared.

The effects of the different length MWCNTs on the dispersion and the nanostructure of cement nanocomposites are shown in Fig. 7. The figure shows SEM images of the fracture surface of the samples reinforced with short and long MWCNTs at two different concentrations at a scale of 1  $\mu\text{m}$ . It can be observed that in all cases MWCNTs seem well dispersed in cement paste and only individual MWCNTs can be identified on the fracture surface.

As it was mentioned before, sonication is a procedure resulting in very high amounts of energy in the mix. While SEM imaging and rheology confirmed that these high levels of energy resulting from sonication were absolutely necessary for adequate dispersion of the MWCNTs, a question arose if sonication can change the performance of the surfactant alone. To address this question the mechanical performance of cement paste samples prepared without surfactant (CP), with surfactant (CP + SFC) and with surfactant sonicated (CP + SFC Sonicated) using the exact same amounts and procedure that was followed for the dispersion of the MWCNTs (Section 2.1) was

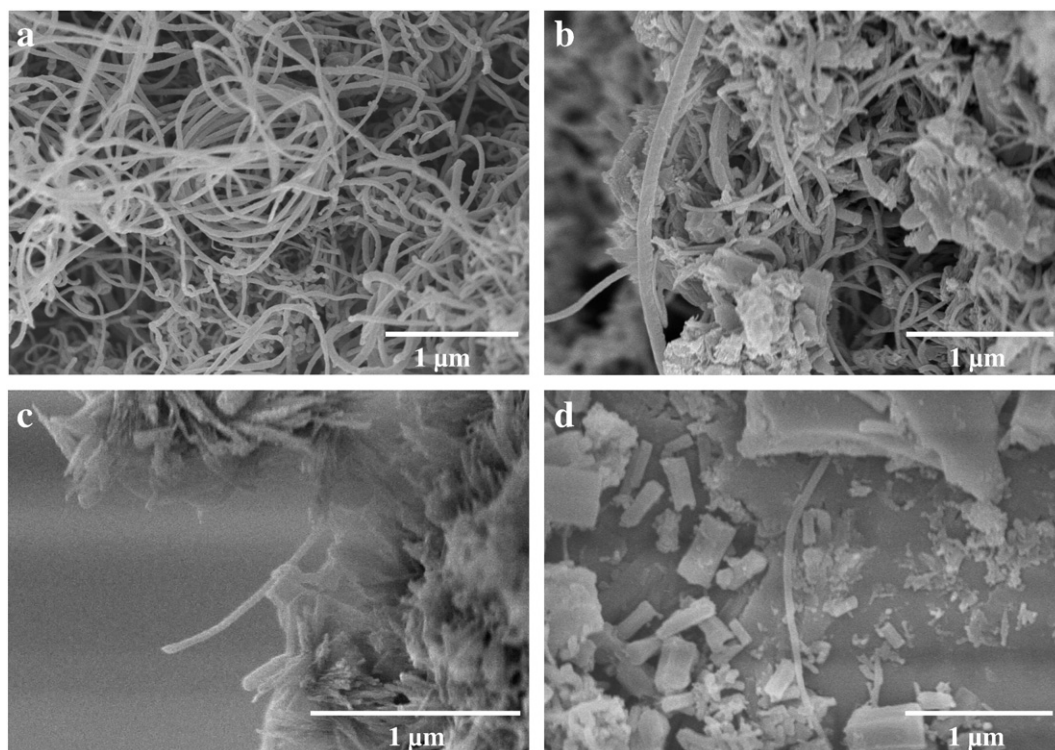


Fig. 5. Surfactant concentration effect on nanotube dispersion: (a)–(d) represent a dispersant to MWCNT weight ratio of 0, 1.5, 4.0 and 6.25, respectively.

investigated. Results of the rate of the flexural strength through the age of 28 days of hydration are shown in Fig. 8. Since no difference in the flexural strength of the samples was observed, plain cement paste was used as the control mix throughout the rest of this research.

The fracture mechanics test results of the flexural strength and the Young's modulus of cement paste samples reinforced with short and long MWCNTs at concentrations of 0.048 wt.% and 0.08 wt.% at the age of 3, 7 and 28 days are presented in Fig. 9(a) and (b), respectively. In all cases, the samples reinforced with MWCNTs exhibit higher flexural strength and Young's modulus than plain cement paste. More specifically, at the age of 3 days the samples with short MWCNTs at an amount of 0.08 wt.% give a higher increase in the flexural strength. Comparing the response of the samples with short MWCNTs with different concentrations it is observed that the samples reinforced with a higher amount of MWCNTs exhibit higher strength and Young's modulus. Different performance is observed with the samples reinforced with long MWCNTs. Samples reinforced with a smaller concentration of MWCNTs demonstrate a higher strength and Young's modulus increase. Comparing the performance of the shorter length MWCNTs nanocomposites with the performance of nanocomposites

with longer MWCNTs it is observed that the highest flexural strength at 3 and 7 days of hydration is obtained with the 0.08 wt.% short MWCNTs followed by the mixes with 0.048 wt.% long MWCNTs (Fig. 9(a)). Samples reinforced with 0.08 wt.% short, 0.048 wt.% and 0.08 wt.% long MWCNTs gave the same 28 day flexural strength. However, looking at Fig. 9(b) it is observed that the highest increase of the Young's modulus is achieved for cement paste nanocomposites reinforced with 0.048 wt.% long and 0.08 wt.% short MWCNTs. Based on the above findings it can be concluded that a higher concentration of short MWCNTs is needed to achieve effective reinforcement while a lower concentration of long MWCNTs is required to attain the same level of mechanical performance. Taking into consideration the cost of MWCNTs, where short MWCNTs are much cheaper than the longer ones, both possibilities are worth exploring.

### 3.4. Reinforcing effect of MWCNTs

Table 3 compares the flexural strength increase of cement paste nanocomposites achieved in this experimental study with results of mortars and cement paste nanocomposites reported in the literature, relative to the concentration of CNTs used. It is observed that a similar gain (25%) in the flexural strength of mortars nanocomposites was obtained by Li et al. [8], using ten times higher concentration of CNTs (0.5 wt.% of cement). Comparing the results of this study with the results obtained by Cwirzen et al [12] it is observed that, despite the similar CNTs concentration used for the preparation of cement paste nanocomposites, the flexural strength increase for Cwirzen et al was 10%. The extent of the flexural strength improvement of the nanocomposites in this work was attributed to the successful nanofiber dispersion. Effective dispersion of the CNTs in the cement matrix resulted in the reduction of the fiber free area in the material and in an increase in the mechanical performance of the nanocomposite. In conclusion, only a small amount of effectively dispersed CNTs is needed to achieve an enhanced reinforcing effect of the cementitious matrix and the production of a low cost nanocomposite.

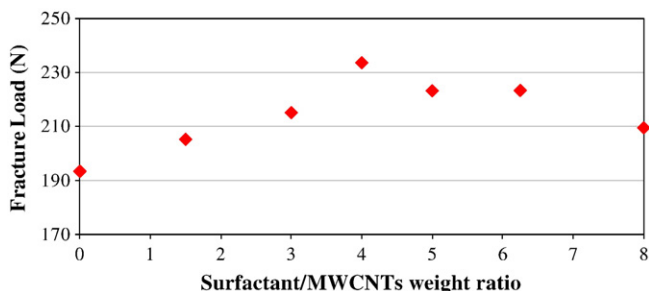


Fig. 6. Fracture load of 28 days w/c = 0.5 cement paste reinforced with long MWCNTs (0.08 wt.% by weight of cement).

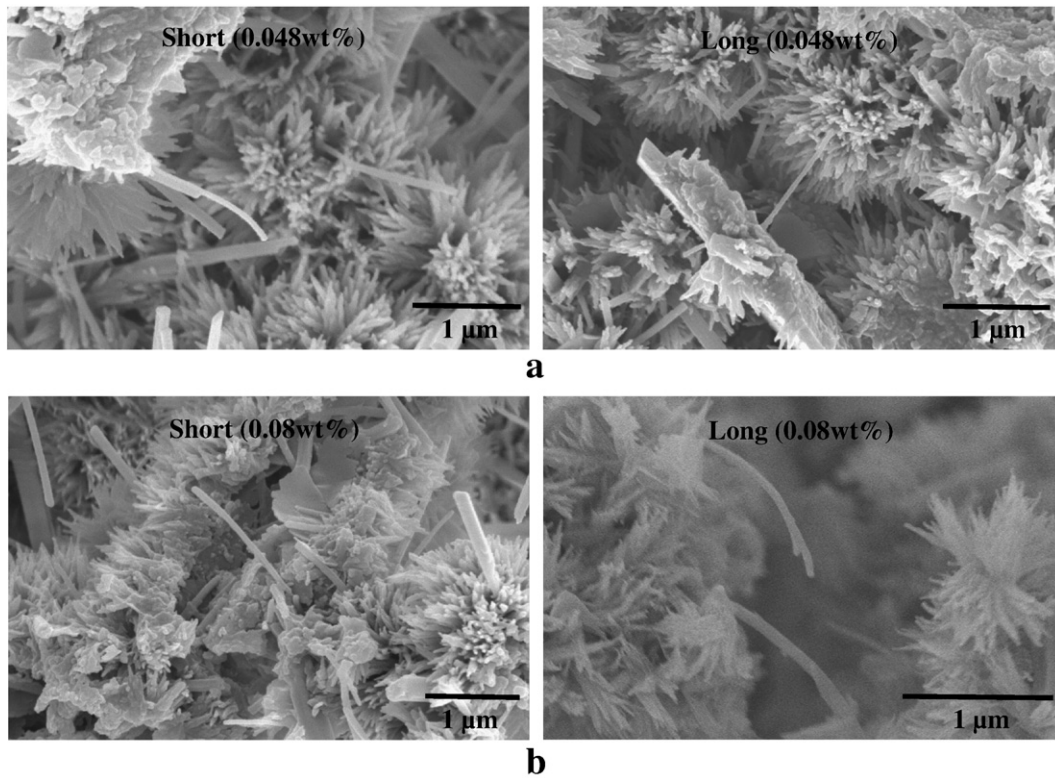


Fig. 7. Effect of different types of MWCNTs (short-long) with concentrations of (a) 0.048 wt.% and (b) 0.08 wt.% in 18 h cement paste.

The Young's modulus of the nanocomposite was increased by 45%. An easy and effective way to predict the upper-bound value for the Young's modulus of a composite material is to use the parallel model. The parallel model describes the modulus of a composite material as a function of the properties of its constituent materials, assuming that the two phases of the composite are subject to uniform strains [22]. The Young's modulus can be calculated by Eq. (1), in which  $E_c$ ,  $E_m$  and  $E_f$  represent the Young's modulus of the nanocomposite, matrix and CNTs, respectively, and  $V_m$  and  $V_f$  are the volume fractions of the matrix and CNTs, respectively.

$$E_c = V_m E_m + V_f E_f \quad (1)$$

Based on Eq. (1), the predicted Young's modulus of cement paste nanocomposite reinforced with 0.08 wt.% short MWCNTs at the age of 28 days is 9.1 GPa. It is observed that the predicted modulus is much lower than the experimental value of 13 GPa. An evaluation study of the Young's modulus of concrete nanocomposites reinforced with 1% CNTs predicts a 33% increase [23], which is lower than the increase obtained in this study. To further investigate the increase of the Young's modulus, nanoindentation tests were performed.

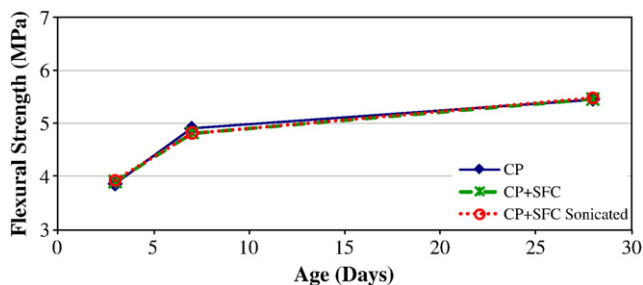


Fig. 8. Flexural strength of cement paste samples prepared without surfactant (CP), with surfactant (CP + SFC) and with surfactant sonicated (CP + SFC Sonicated).

### 3.5. Nanoindentation

In order to investigate the effect of MWCNTs on the nanomechanical properties of the cementitious nanocomposites, nanoindentation tests were performed on 28 days cement paste samples reinforced with 0.08 wt.% short MWCNTs. Fig. 10 shows the probability plot of the Young's modulus of cement paste reinforced with MWCNTs ( $w/c = 0.5$ ).

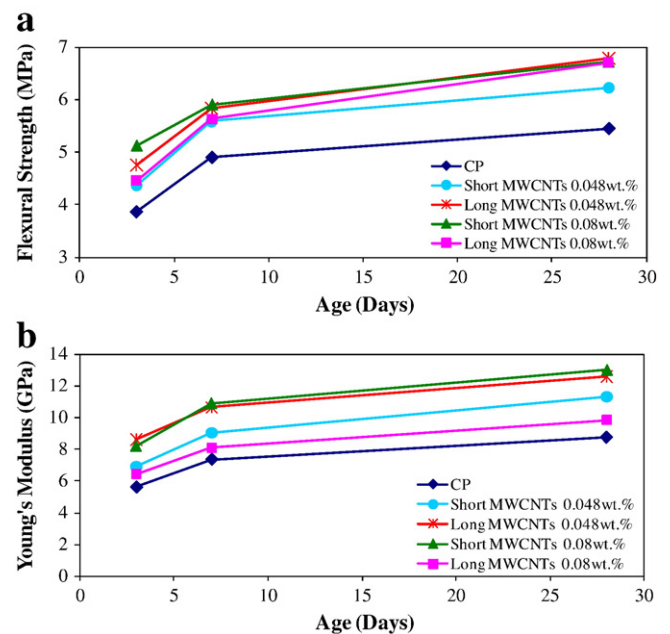


Fig. 9. Effect of different types (short and long) of MWCNTs and concentration on (a) the flexural strength and (b) the Young's modulus of cement paste ( $w/c = 0.5$ ).



**Table 3**

Comparison of flexural strength increase in cementitious nanocomposites reinforced with CNTs.

Researchers	Nanocomposites	Amount of CNTs (wt.% of cement)	Flexural strength increase (%)
Li (2005) [8]	Mortars	0.50	25
Cwirzen (2008) [12]	Cement paste	0.042	10
Konsta-Gdoutos et al. [present work]	Cement paste	0.08 and 0.048	25

Similar experiments, using the same type of cement and testing procedure, were carried out by Mondal [24] on 28 days cement paste specimens ( $w/c = 0.5$ ), who used a peak analyzing protocol to fit four normal distributions to the probability plot of the Young's modulus corresponding to the porous phase, low stiffness C–S–H, high stiffness C–S–H and calcium hydroxide. The same analyzing protocol was used by Constantinides and Ulm [25] on the nanoindentation results of 5 months white cement paste specimens ( $w/c = 0.5$ ). The probability plot of Young's modulus of cement paste reinforced with MWCNTs is in agreement with the probability plot of Mondal [24] and the frequency plot of Constantinides and Ulm [25]. However, while the peak of the distribution of the nanoindentation modulus of both Mondal [24] and Constantinides and Ulm [25] falls in the area of 15 to 20 GPa and represents the low stiffness C–S–H, the peak of the probability plot of the Young's modulus of the MWCNT nanocomposite was found to be in the area of 20–25 GPa which represents the high stiffness C–S–H. This result suggests that the incorporation of MWCNTs increased the amount of high stiffness C–S–H. Similar results were obtained with nanosilica cement composites by Gaitero [26]. Furthermore, the area between 0 to 15 GPa is attributed to a material region for which the indentation response is dominated by high porosity. Comparing the probability plot of the Young's modulus of the MWCNTs nanocomposite with the results of Mondal [24] it is observed that the probability of Young's modulus below 10 GPa is reduced from 0.10 to 0.03 in the case of the samples with MWCNTs. These results suggest that MWCNTs reduce the nanoporosity of cement paste by filling the gaps between the C–S–H gel. This result also agrees well with the experimental results of Li et al. [8]. Further testing however, is on the way to elucidate those findings.

#### 4. Conclusions

The rheological properties, the macro- and nanoscale mechanical properties and the nanostructure of the cement nanocomposites reinforced with MWCNTs have been investigated. Effective dispersion was achieved by applying ultrasonic energy and with the use of a surfactant. Results have shown that for proper dispersion, the application of ultrasonic energy is required. The combination of the SEM and fracture mechanics test results suggests that for effective dispersion, a weight ratio of surfactant to MWCNT close to 4.0 is

required. The fracture mechanics test results indicate that the fracture properties of cement matrix increased through proper dispersion of small amounts of MWCNTs (0.048 wt.% and 0.08 wt.%). In particular, higher concentrations of short MWCNTs are required to achieve effective reinforcement, while lower amounts of longer MWCNTs are needed to achieve the same level of mechanical performance. The nanoindentation results suggest that MWCNTs can strongly reinforce the cement paste matrix at the nanoscale by increasing the amount of high stiffness C–S–H and decreasing the porosity.

#### Acknowledgements

The authors would like to acknowledge the financial support from the Infrastructure Technology Institute at Northwestern University under Grant DTRT06-G-0015/M1. The scanning electron microscopy experiments were carried out in the EPIC facility of NUANCE center at Northwestern University. The nanoindentation experiments were carried out in the NIFTI facility of NUANCE center at Northwestern University with the help of Dr. Paramita Mondal whose advice and suggestions are gratefully acknowledged.

#### References

- [1] Y. Akkaya, S.P. Shah, M. Ghandehari, Influence of fiber dispersion on the performance of microfiber reinforced cement composites, *ACI Special Publications* 216: Innovations in Fiber-Reinforced Concrete for Value, SP-216-1, 216 (2003) 1–18.
- [2] J.M. Makar, J.J. Beaudoin, Carbon nanotubes and their applications in the construction industry, in: P.J.M. Bartos, J.J. Hughes, P. Trtik, W. Zhu (Eds.), *Nanotechnology in construction*, Proceedings of the 1st International Symposium on Nanotechnology in Construction, Royal Society of Chemistry, 2004, pp. 331–341.
- [3] M.S. Konsta-Gdoutos, Z.S. Metaxa, S.P. Shah, Multi-scale mechanical and fracture characteristics and early-age strain capacity of high performance carbon nanotube/cement nanocomposites, *Cem. Concr. Comp.* 32 (2) (2010) 110–115.
- [4] S.P. Shah, M.S. Konsta-Gdoutos, Z.S. Metaxa, P. Mondal, Nanoscale modification of cementitious materials, nanotechnology in construction 3, in: Z. Bittnar, P.J.M. Bartos, J. Nemecek, V. Smilauer, J. Zeman (Eds.), *Proceedings of the Third International Symposium on Nanotechnology in construction*, Springer, 2009, pp. 125–130.
- [5] J.P. Salvetat, J.M. Bonard, N.H. Thomson, A.J. Kulik, L. Forro, W. Benoit, et al., Mechanical properties of carbon nanotubes, *Appl. Phys. A* 69 (3) (1999) 255–260.
- [6] T. Belytschko, S.P. Xiao, G.C. Schatz, R. Ruoff, Atomistic simulations of nanotube fracture, *Phys. Rev. B* 65 (23) (2002) 235430–235437.
- [7] J.M. Makar, J. Margeson, J. Luh, Carbon nanotube/cement composites – early results and potential applications, *Proceedings of the 3rd International Conference on Construction Materials: Performance, Innovations and Structural Implications*, Vancouver, B.C., Canada, 2005 pp.1–10.
- [8] G.Y. Li, P.M. Wang, X. Zhao, Mechanical behavior and microstructure of cement composites incorporating surface-treated multi-walled carbon nanotubes, *Carbon* 43 (6) (2005) 1239–1245.
- [9] G.Y. Li, P.M. Wang, X. Zhao, Pressure-sensitive and microstructure of carbon nanotube reinforced cement composites, *Cem. Concr. Comp.* 29 (5) (2007) 377–382.
- [10] Y. Saez de Ibarra, J.J. Gaitero, E. Erkizia, I. Campillo, Atomic force microscopy and nanoindentation of cement pastes with nanotube dispersions, *Physica Status Solidi (a)* 203 (6) (2006) 1076–1081.
- [11] S. Wansom, N.J. Kidner, L.Y. Woo, T.O. Mason, AC-impedance response of multi-walled carbon nanotube/cement composites, *Cem. Concr. Comp.* 28 (6) (2006) 509–519.
- [12] A. Cwirzen, K. Habermehl-Chirzen, V. Penttala, Surface decoration of carbon nanotubes and mechanical properties of cement/carbon nanotube composites, *Adv. Cem. Res.* 20 (2) (2008) 65–73.
- [13] N. Groert, Carbon nanotubes becoming clean, *Mater. Today* 10 (1–2) (2007) 28–35.
- [14] X.L. Xie, Y.W. Mai, X.P. Zhou, Dispersion and alignment of carbon nanotubes in polymer matrix: a review, *Mater. Sci. Eng. Rep.* 49 (4) (2005) 89–112.
- [15] Y. Yang, A. Grulke, G.Z. Zhang, G. Wu, Thermal and rheological properties of carbon nanotube-in-oil dispersions, *J. Appl. Phys.* 99 (11) (2006) 114307.
- [16] S.P. Shah, S.E. Swartz, C. Ouyang, *Fracture mechanics of concrete: application of fracture mechanics to concrete, rock and other quasi-brittle materials*, John Wiley and Sons, New York, 1995.
- [17] J. Nemecek, L. Kopecky, Z. Bittnar, Size effect in nanoindentation of cement pastes, in: Y. de Miguel, A. Porro, P.J.M. Bartos (Eds.), *Proceeding of the 2nd International Symposium in Nanotechnology*, RILEM Publications SARL, 2006, pp. 161–168.
- [18] W.C. Oliver, G.M. Pharr, An improved technique for determining hardness and elastic modulus using load and displacement sensing indentation experiments, *J. Mater. Res.* 7 (1992) 1564–1583.

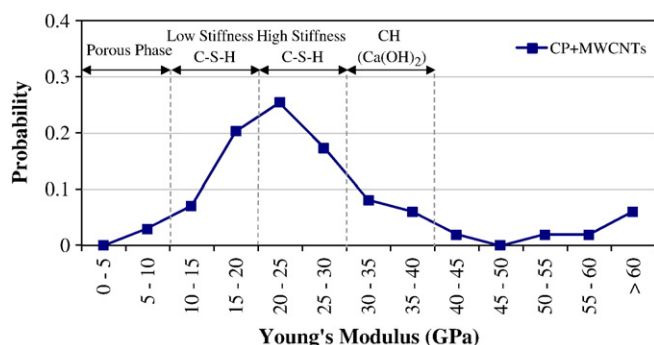


**Fig. 10.** Probability plot of the calculated Young's modulus of 28 day cement paste reinforced with 0.08wt.% short MWCNTs ( $w/c = 0.5$ ).

- [19] Z.S. Metaxa, M.S. Konsta-Gdoutos, S.P. Shah, Carbon nanotubes reinforced concrete, *ACI Special Publications* 267: Nanotechnology of Concrete: The Next Big Thing is Small, SP-267-2, 267 (2009) 11–20.
- [20] Y. Junrong, N. Grossiord, C.E. Koning, J. Loos, Controlling the dispersion of multi-wall carbon nanotubes in aqueous surfactant solution, *Carbon* 45 (3) (2007) 618–623.
- [21] T. Hielscher, Ultrasonic production of nano-size dispersions and emulsions, *Proceedings of 1st Workshop on NanoTechnology Transfer in Europe*, TIMA Editions, Grenoble, France, 2006, pp. 138–143.
- [22] S. Mindess, J.F. Young, D. Darwin, *Concrete*, Prentice Hall, Upper Saddle River, 2003.
- [23] G. Rouainia, K. Djeghaba, Evaluation of Young's modulus of single walled carbon nanotube (SWCNT) reinforced concrete composite, *J. Eng. Appl. Sci.* 3 (2008) 504–515.
- [24] P. Mondal, Nanomechanical properties of cementitious materials, PhD thesis, Northwestern University (2008).
- [25] G. Constantinides, F.-J. Ulm, The nanogranular nature of C–S–H, *J. Mech. Phys. Solids* 55 (1) (2007) 64–90.
- [26] J.J. Gaitero, Multi-scale study of the fiber-matrix interface and calcium leaching in high performance concrete, PhD thesis, Labein-Technalia (2008).